UCRL-JC-131212
PREPRINT

Single-Beam Photothermal Microscopy - A New Diagnostic Tool for Optical Materials

Z. L. Wu, M. D. Feit, M. Kozlowski,
J. Y. Natoli, A. M. Rubenchik,
L. Sheehan, and M. Yan

This paper was prepared for submittal to the
30th Boulder Damage Symposium: Annual Symposium on
Optical Materials for High Power Lasers
Boulder, Colorado
September 28 - October 1, 1998

December 22, 1998

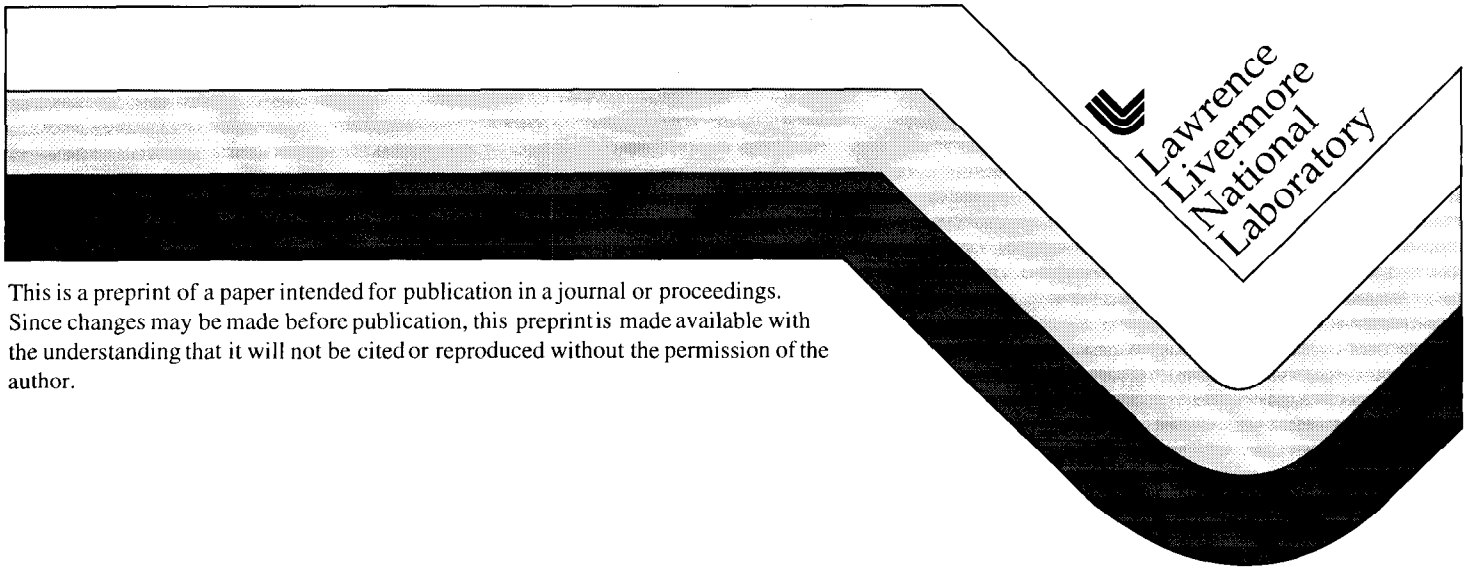

Single-beam photothermal microscopy - a new diagnostic tool for optical materials

Z. L. Wu, M. D. Feit, Mark Kozlowski, J. Y. Natoli, A. M. Rubenchik, L. Sheehan, and M. Yan
Lawrence Livermore National Laboratory
University of California, Livermore, CA 94550

ABSTRACT

A novel photothermal microscopy (PTM) is developed which uses only one laser beam, working as both the pump and the probe. The principle of this single-beam PTM is based on the detection of the second harmonic component of the laser modulated scattering (LMS) signal. This component has a linear dependence on the optical absorptance of the tested area and a quadratic dependence on the pump laser power. Using a pump laser at the wavelengths of 514.5- and 532-nm high-resolution photothermal scans are performed for polished fused silica surfaces and a HfO_2/SiO_2 multilayer coatings. The results are compared with those from the traditional two-beam PTM mapping. It is demonstrated that the single-beam PTM is more user-friendly (i.e. no alignment is needed) than conventional two-beam PTM and, offers a higher spatial resolution for defect detection.

Keywords: single beam photothermal microscopy, laser modulated scattering, nondestructive evaluation, characterizations of defects, laser-induced damage, optical surfaces and thin film coatings

1. Introduction

The development of high power optics for the National Ignition Facility (NIF) requires diagnostic tools to meet new challenges. First, a high spatial resolution is needed to detect sub-micron defects and micro-cracks, as conceptually illustrated in Figure 1. For finished fused silica surfaces these defects play an important role in the UV laser (3 ns, 355 nm) damage process [1-3]. Second, the applicability to large-area sampling is needed, since the NIF optical components are large-aperture (up to 0.34 m^2) in nature. Finally, it is desirable that they can be used for studying rough (i.e. damaged) surfaces, since the laser damage concern of NIF requires an understanding of the damage growth behavior of previously damaged sites so as to correctly predict the life time of NIF optics [4].

A number of techniques have been introduced to investigate localized defects in optical materials, including scanning tools such as atomic force microscopy [5,6] and near field scanning optical microscope [7,8], and imaging tools including optical microscope and total internal reflection microscopy [9,10]. Photothermal microscopy (PTM) [11-16], with the capacity to directly address absorption and thermo-mechanical response issues relevant to laser damage, has also been widely used, in particular for thin film coatings. Previous studies have demonstrated that PTM can locate relevant defects and correlate well with laser damage studies [16,17].

Most PTMs, however, use a pump-probe strategy that uses a two-beam geometry, as illustrated in Figure 2 (a) for a PTM based on photothermal deflection effect [11-15]. The two-beam PTM as shown has a few fundamental limitations. First, the photothermal signal is very sensitive to the relative position of the pump and probe beams [11] and hence an accurate alignment is needed for each measurement. Its practicality for manufacturing environment and high-resolution scanning for large aperture optics is therefore limited. Second, mechanical interference between the optics needed for constructing the PTM does not allow the achievement of an ultra-high spatial resolution (sub-micron) without a substantial complication of the design. Third, most two-beam PTMs are based on photothermal deflection and/or diffraction effects and are bright-field microscopic tools, as illustrated in Figure 2 (b). There is a PTM signal even for a defect free area, as long as it absorbs the pump laser energy and causes local temperature rise and surface deformation. Therefore for a small defect with a size much smaller than the pump or probe laser beam size, its contribution to the overall photothermal signal can be overwhelmed by the background contribution from the host material. Finally, for studying an already-damaged site, the traditional two-beam PTMs are not suitable, since the strong scattering of the damage site destroys the quality of the reflected probe beam.

To complement the existing defect inspection/characterization techniques and overcome some of their limitations, a single-beam PTM instrument has been developed based on the detection of the second harmonic component of the laser modulated scattering (LMS) signal [18]. LMS allows simultaneous measurement of the optical scattering and photothermal response of localized defects and therefore can help differentiate absorptive defects from non-absorptive ones. LMS is also in principle a dark-field tool for defect detection on optical surfaces since no other parts of a super-polished optics but the defect sites generate scattering signal [18]. By introducing the single-beam detection scheme to the LMS technique, the requirement of an accurate beam alignment is eliminated since there is only one laser beam involved. Other potential advantages of the single-beam PTM include its high sensitivity to small defects even with large beam sizes and its potential applications to the study of photothermal properties of laser damage sites and real-time monitoring of laser damage growth.

This paper briefly describes the experimental method for the single-beam PTM, summarizes the preliminary results that serve as a feasibility study, and discusses the advantages and limitations of the LMS-based single-beam PTM for surface and subsurface defect inspection in optical materials.

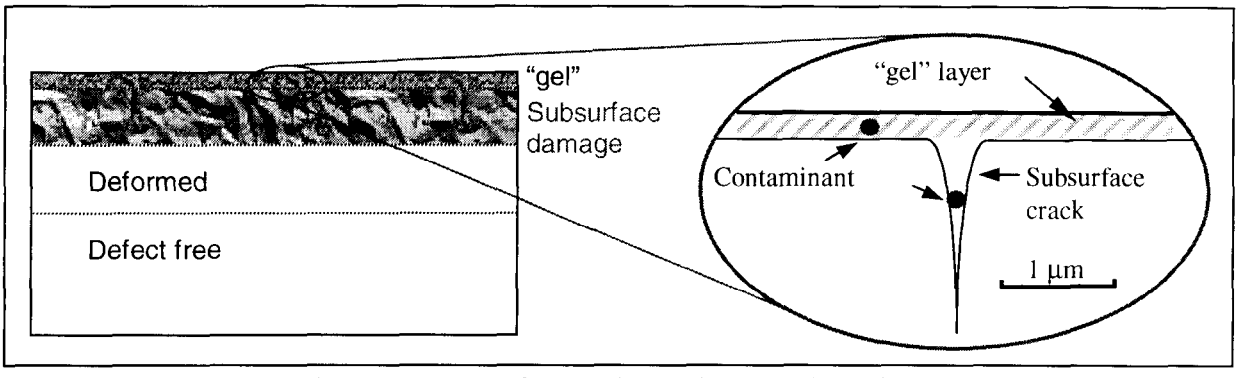

Figure 1. Illustration of the layered structure of sub-surface regime of polished fused silica. The thickness of the different layers shown differ from process to process, but typically the "gel" layer (re-deposition layer during the polishing process) is at the order of 10 - 100 nm, the subsurface damage layer 1 - 100 μm, and the deformed layer 1- 200 μm [3].

2. Experimental method

The operational principle of the single-beam PTM is illustrated in Figure 3 (a). An intensity modulated pump beam is used to irradiate the sample, and the scattered light of the pump laser from the sample surface is used as the probe for local defects. The absorption of the pump beam energy by the sample causes a localized temperature rise and a surface thermal deformation. Depending on the thermal properties of the sample as well as the modulation frequency and beam size of the pump beam, the lateral dimension of the locally heated / thermal deformed area can range from a few microns to millimeters. For a typical PTM operation on defect-free areas of fused silica surfaces or optical thin film coatings, the dimensions of the surface deformation are in the range of subnano- to nano-meters for the vertical direction and tens to hundreds microns laterally [19]. Such a deformation in surface shape may cause detectable changes in the beam profile of the specular reflection, but it is unimportant to the scattering field detected at an angle far from the angle of specular reflection [20]. The scattering field is more sensitive to localized variation of optical index.

For a sinusoidal modulation of the incident pump beam, the detected scattering signal has a first harmonic signal that represents the conventional scattering of the sample and a second harmonic signal that is thermally modulated, i.e. a photothermal signal. Both harmonics can be detected using the lock-in technique. Mapping of an optic can be achieved by either scanning the sample or using a detector array. For the scanning case, the resolution is determined by the size of the pump laser beam. When imaging using a focal array detector, the pixel size of the image is the limiting factor for the spatial resolution.

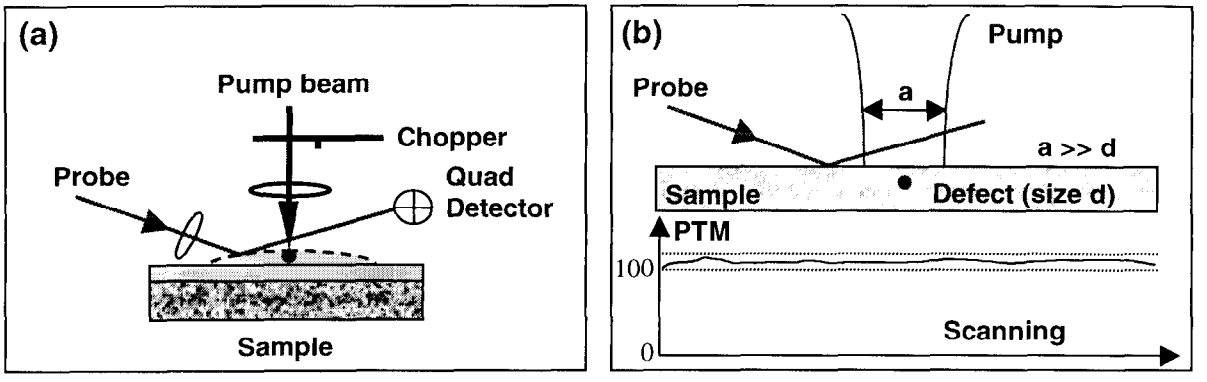

Figure 2. (a) Illustration of the operational principle of a typical two-beam PTM based on photothermal deformation effect [11]. For such a system an accurate alignment of the relative position of the pump and probe beams on the sample surface is required. (b) A conceptual illustration to show that the two-beam PTM based on photothermal deformation effect is a bright-field microscope, i.e. there is a PTM signal even for a defect free area, as long as it absorbs the pump laser energy. Therefore for a small defect with a size much smaller than the pump beam size its contribution to the overall photothermal signal can be overwhelmed by the background signal from the host material.

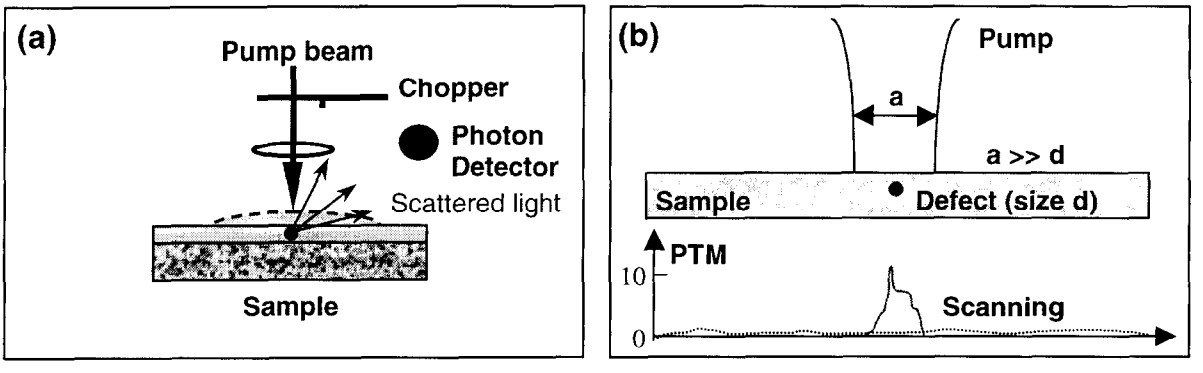

Figure 3. (a) Illustration of the operational principle of a single-beam PTM based on LMS [17]. Since there is only one laser beam involved there is no need for an accurate alignment of the system. In this case the scattered slight is detected rather than a specular reflection light. Signal will only be detected from defect sites, thus making it a dark-field technique. (b) A conceptual illustration of single-beam PTM data showing that the background signal is depressed revealing the signal for the defect site.

Note that the spatial resolution should not be confused with the sensitivity of the technique for detecting small-size defects. The latter depends on the magnitude of the signal at defect site relative to the background, not the physical size of the defect. For single-beam PTM based on LMS, the signal from a perfect surface is zero since there is no scattering, therefore its sensitivity to local defects on or underneath a super-polished surface can be extremely high, as conceptually illustrated in Figure 3(b).

The experimental system for performing single-beam PTM is optically depicted in Figure 4. The system is designed such that it can operate at both single-beam and two-beam PTM modes. For the two-beam PTM mode, a 633 nm He-Ne probe laser is used for detecting the surface deformation generated by the 532 nm diode pumped solid state laser. For the single-beam PTM mode, the probe beam is turned off, and the scattered light of the 532 nm laser is used as the probe. Correspondingly, the narrow-band filter in front of the detector is also changed from 633 nm to 532 nm. For both operational modes the detector is placed at about 60° from the normal incidence angle. The lock-in amplifier can be set for either the 1st or the 2nd harmonic signal. By using two lock-in amplifies the 1st and 2nd harmonic signals can be measured simultaneously.

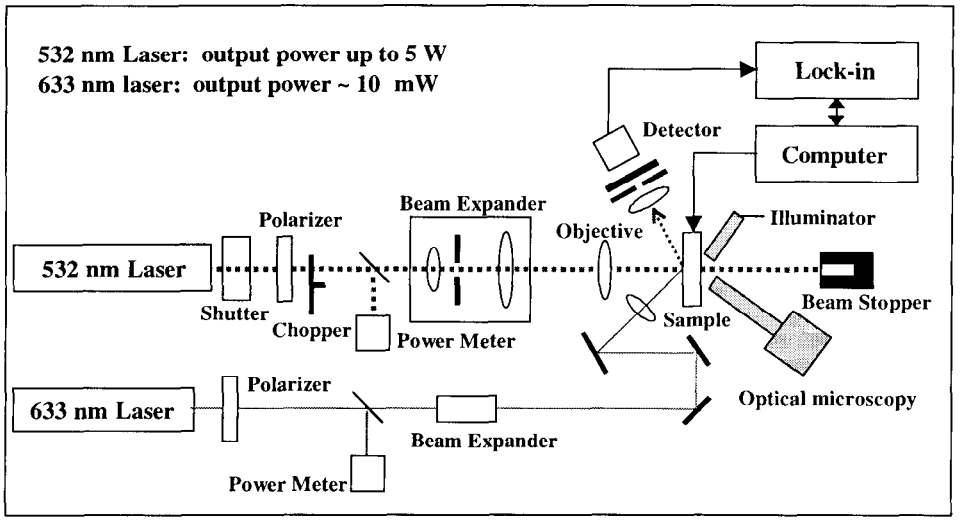

Figure 4. Optical depiction of the experimental setup for PTM. The system is designed such that it can operate at both single-beam and two-beam PTM modes. For the single-beam mode, the 633 nm probe beam is blocked and the scattered light of the 532 nm laser is used as the probe. For the two-beam mode, the specular reflection of the 633 nm laser is used as the probe. For details see text.

The system illustrated in Figure 4 is used mainly for high-resolution scanning for optical thin film coatings. Its pump beam diameter is at the order of about 5 μm, and the probe beam is about 3-5 times larger than the pump beam. For some of the experimental efforts the laser wavelength and the size of the pump beam are modified. For example, an Argon-ion laser is frequently used to replace the 532 nm solid state laser for more choices of the pump laser wavelengths. For the experimental results presented in this paper, specific experimental parameters are stated for each curve and/or image.

3. Results and discussion

Optical scattering from a small defect / particle in general is a complicated phenomenon [21]. The understanding of the second harmonic signal is further complicated by the transient nature of the photothermal response of an unknown defect and the resulting modification to the scattering field. While a detailed modeling of single-beam PTM is in progress, an analytical model based on the perturbation method shows that the first harmonic scattering signal is proportional to the pump laser power, and the second harmonic to the square of pump power [20]. Experimentally both the linear and the quadratic relationships are verified when the pump laser power is at appropriate levels, as shown in Figure 5 by results obtained for a micro-damage site (~5 μm) on a Nd:glass surface. When the pump power goes to higher levels, high-order nonlinear response dominates the 2^{nd} harmonic signal while the linear relationship between the 1^{st} harmonic signal and the pump power is maintained untill laser damage happens at about 900 mW (pump beam size ~ 100μm). It is interesting to note that the high-order nonlinear response of the 2^{nd} harmonic signal occurs well below the damage threshold of the defect site, as shown in Figure 5(b). The mechanism of this high-order nonlinear signal is not understood at this time.

The signal shown in Figure 5 (b) can be roughly divided in three zones. Zone 1 is the safe zone, where the 2^{nd} harmonic signal behaves as predicted and is proportional to the square of the pump power. Zone 2 is the caution zone, where the high-order nonlinear response is not understood at this time, and it may be related with both the nonlinear properties of the sample and the diagnostic method. Zone 3 is the damage zone, where the 2^{nd} harmonic signal becomes unstable and not reproducible and laser damage to material may be occurring. For the image shown later in this paper, all the operation are done with pump power levels within the safe zone, so that interpretation of the signal is more straight forward.

The quadratic relationship between the 2nd harmonic signal and the pump laser power make it easier to obtain high-amplitude signals even for low absorptive materials. While this is a good feature in terms of signal enhancement, caution should be taken to interpret the data. For example, the 2nd harmonic signal needs to be normalized against the 1st harmonic signal to eliminate any contribution from topographical features. The normalized 2nd harmonic signal is proportional to the level of the absorbed pump laser energy. Therefore, scanning an optical surface by using a constant pump laser power maps absorption of the surface if the 2nd harmonic signal is normalized to the 1st harmonic scatter signal. For the images presented in this paper, all of the single-beam PTM images have been normalized against their corresponding 1st harmonic image, or scatter map.

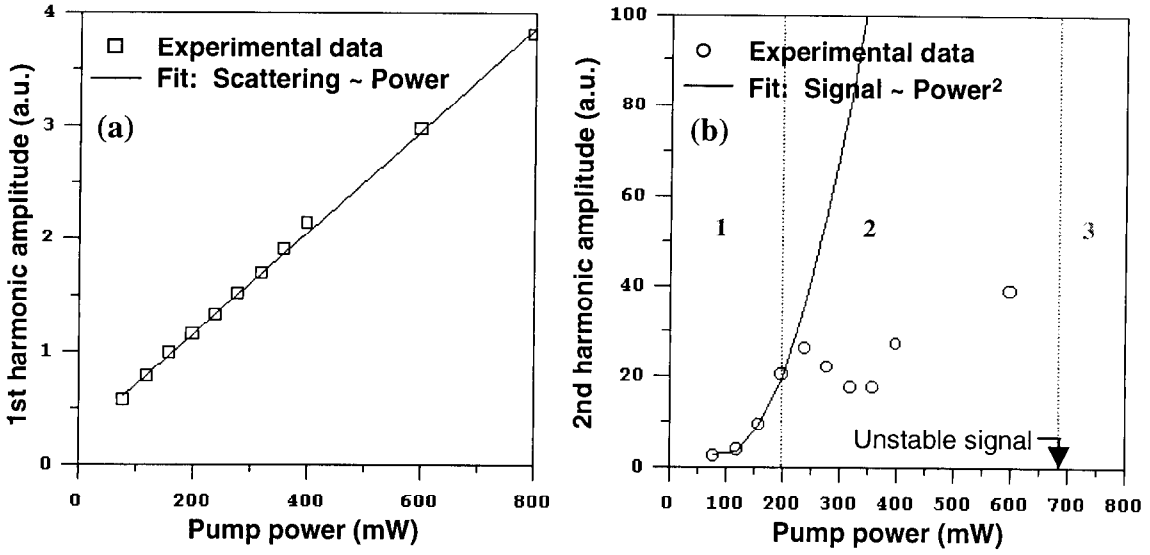

Figure 5. (a) The 1st harmonic scattering signal as a function of the pump laser power. (b) The 2nd harmonic scattering signal as a function of the pump laser power. The sample used is a micro-damage site (with a size of about 5 μm) on the surface of laser glass. Three zones are shown in the data. Zone 1 – safe zone: the 2nd harmonic signal behaves as predicted and is proportional to the square of the pump power. Zone 2 – caution zone: the high-order nonlinear response is not understood at this time, and it may be related with the nonlinear properties of the materials. Zone 3 – damage zone: the 2nd harmonic signal becomes unstable and laser damage to material may occur. Experimental parameters for both curves are as follows. Pump laser - wavelength 532 nm, beam size ~100μm, normal incidence, chopping frequency 70 Hz; Detector - pinhole size ϕ1.0 mm, 7.5 cm from the heating spot and 60° from the normal of the sample, detecting forward scattering of the pump beam from the reflection mode as shown in Figure 3.

Scatter map and the single-beam PTM images as described above were obtained for a variety of samples. Figure 6 is the scatter map (the 1st harmonic signal) and its profile along the line labeled A1-A1, obtained on a fused silica surface using a 514.5 nm Argon-ion laser. Quite a few defect sites are detected, as shown in both the amplitude and the phase images. Along the line A1-A1 the signal enhancement at the defect sites is found to be about a factor of 2 for the amplitude map. For the phase map the defect sites deviate from the average background by only a few degrees. Figure 7 provides single-beam PTM maps of the same region imaged in Figure 6. A comparison between Figure 6 and Figure 7 offers insight into the issue of laser damage precursors and help separate absorptive defects from non-absorptive ones. For example, along the profile line A1-A1 in Figure 7, it is found that the maximum photothermal signal enhancement occurs at defect A. The enhancement factor is about 10 for the amplitude map, indicating that defect A is a highly absorptive defect. In the phase map defect A deviates from the average background by about 100 degrees, indicating a strong thermal discontinuity at the defect site. It is likely that defect A is more susceptible to laser damage than defect B, even though the latter is a larger and more scattering defect, as shown in Figure 6. Quantitative understanding of these images and their implications to laser damage, however, needs further work, including the development of a rigorous model for inversion calculation that goes beyond the scope of this paper.

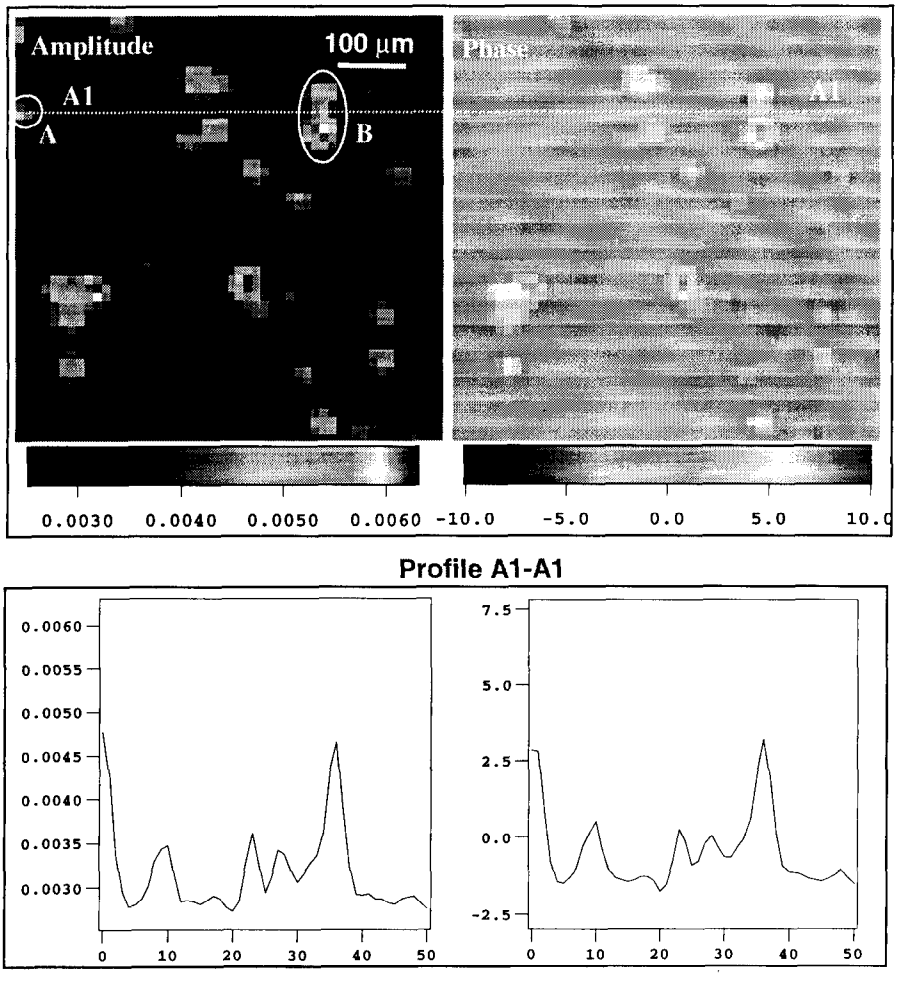

Figure 6. Scattering map (up) and the profile along the A1-A1 line (bottom) for a polished fused silica surface. The amplitude map is in arbitrary unit, and the unit of the phase is degree. The experimental parameters are as follows. Pump laser - wavelength 514.5 nm, beam size ~100 μm, normal incidence, chopping frequency 70 Hz; Detector - pinhole size ϕ1.0 mm, 7.5 cm from the heating spot and 60° from the normal of the sample, detecting forward scattering of the pump beam from the reflection mode as shown in Figure 3.

To further demonstrate the interesting features of single-beam PTM, an nodule defect in a multilayer HfO_2/SiO_2 coating is selected for high-resolution (~5 μm pump beam diameter and 1 μm scanning step-length) scanning. Figure 8 shows the results for the same scanning area but using different techniques as shown in Figure 4, i.e. scattering map, two-beam PTM map, and single-beam PTM map. The scattering map is shown in Figure 8(a). The amplitude is sensitive to geometrical and optical index inhomogenieties as determined by the scattering law. In Figure 8(a) the amplitude image of the scattering map reveals the nodule defect, but contains little information relevant to laser damage. The phase image of the scattering map is almost constant and shows no feature, as would be expected.

The two-beam PTM map of the same area is shown in Figure 8(b). The amplitude image is primarily an absorption map at the low modulation frequency of 70 Hz used in this experiment [22]. It reveals that the nodule is more absorptive than the host thin film coating, as demonstrated by a signal enhancement factor of about 3-4 at the defect site. It is also noted that the phase image contains observable features at the defect site, indicating that there is also a thermal inhomogeneity there. Other observations include that the two-beam PTM is a bright field technique, since both the defect site and defect-free region have substantial photothermal signals. Furthermore, in the two-beam PTM mode the spatial resolution has more limiting factors, including a finite probe beam size.

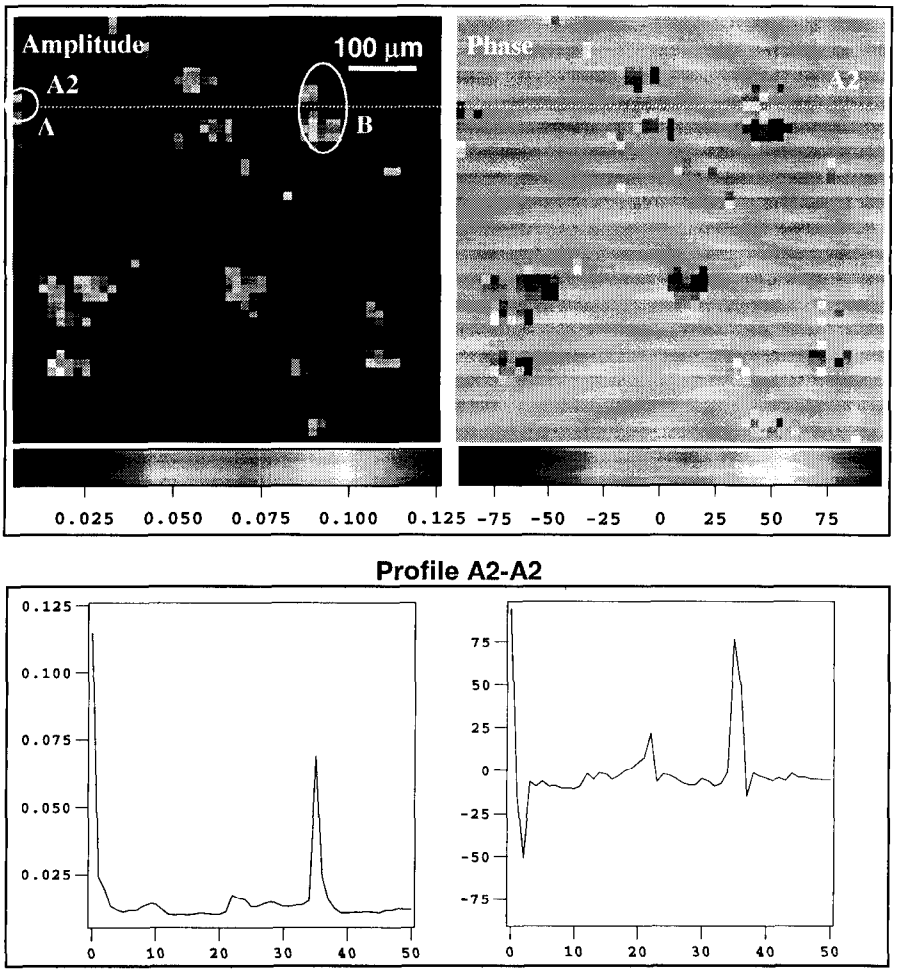

Figure 7. Single-beam PTM image (up) and the profile along the A2-A2 line (bottom) for a polished fused silica surface. The amplitude map is in arbitrary unit, and the unit of the phase is degree. The experimental parameters are as follows. Pump laser - wavelength 514.5 nm, beam size ~100 μm, normal incidence, chopping frequency 70 Hz; Detector - pinhole size ϕ1.0 mm, 7.5 cm from the heating spot and 60° from the normal of the sample, detecting forward scattering of the pump beam from the reflection mode as shown in Figure 3.

The single-beam PTM of the same region is shown in Figure 8(c). The first thing observed is that the single-beam PTM is a dark-field technique, as shown by the amplitude image, where the signal at defect free region is almost negligible. The noisy phase signal at the defect-free region is in coincidence with the low amplitude signal, further demonstrating the dark-field feature of the technique. Secondly, the amplitude image shows that the pump laser-induced "hot" area of the defect site is very localized, with a size of ~(2-3) μm in width and ~9 μm in length. Both the scatter and the two-beam PTM maps show substantially larger features. This result suggests that absorptance of this nodule defect is spatially confined, qualitatively in agreement with previously published electric-field enhancement model for such defects. It also demonstrates that under similar experimental conditions the single-beam PTM has a substantially higher spatial resolution. Thirdly, the phase image shows a phase difference up to 200 degrees between the center of the defect and the defect-free region, indicating again a localized thermal inhomogeneity, and/or depth information of the absorbing center.

Finally, it should be pointed out that the two-beam PTM detects the wavefront distortion of the probe beam caused by the pump laser-induced surface deformation. It is an integrated effect of absorption, heat conduction, thermo-elastic expansion, and optical diffraction. In comparison, single-beam PTM detects laser-modulated scattering that is primarily sensitive to local temperature rise. Therefore, the inversion calculation can be relatively easier.

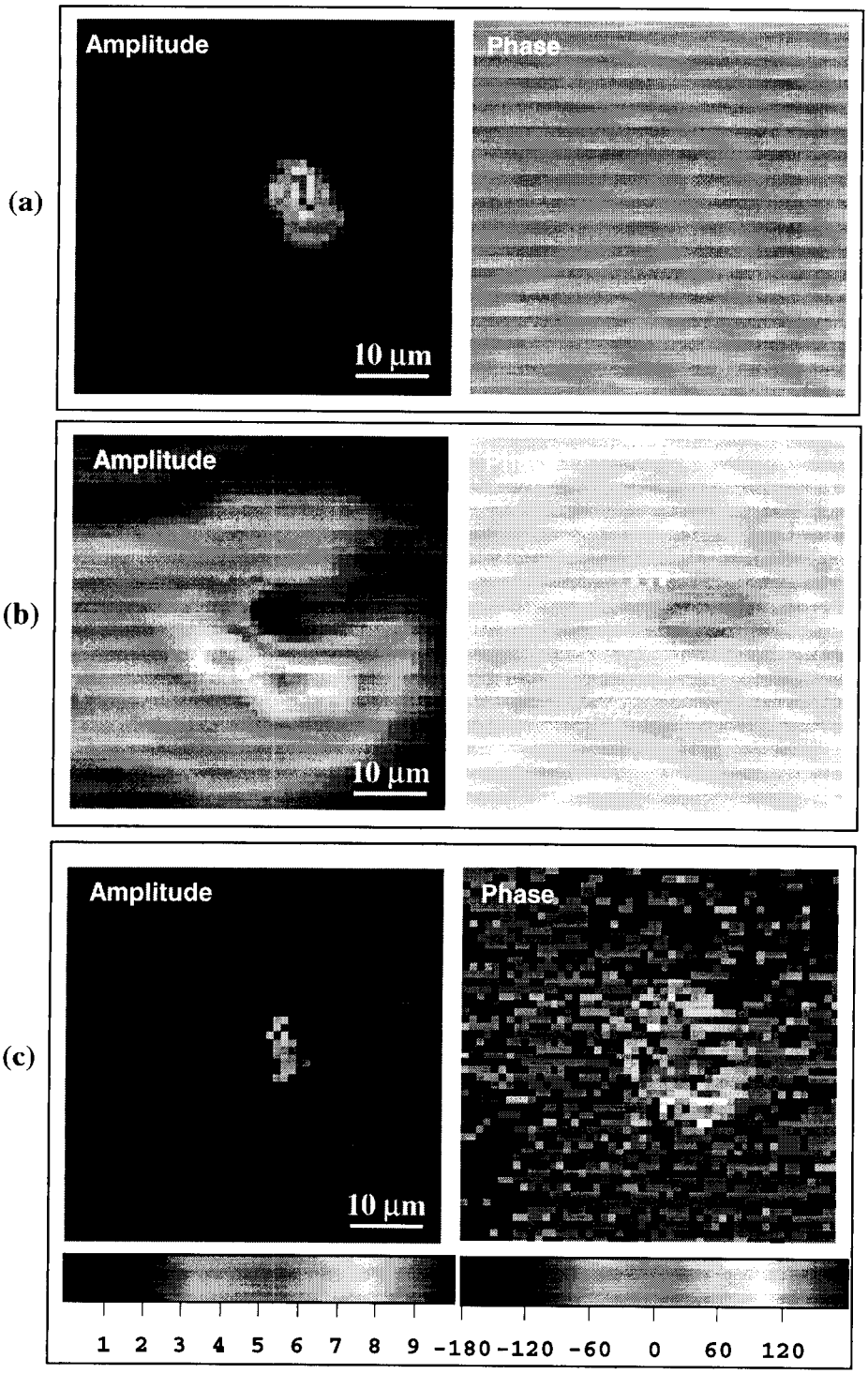

Figure 8. Various imaging results for a same nodule defect in a HfO_2/SiO_2 high-reflection coating using different imaging methods. (a) Scattering map, note that the defect does not show up in the phase image. (b) Two-beam PTM image. (c) Single-beam PTM image. The amplitude images (left column) are normalized and in arbitrary units, and the unit of the phase images are degrees. The experimental parameters are as follows. Pump laser - wavelength 532 nm, beam size ~5 μm, normal incidence, chopping frequency 70 Hz; Detector - pinhole size ϕ1.0 mm, placed at about 60° from the normal of the sample with a lens in front of it to collect the scattered light. The light detected in (a) and (c) is forward scattering of the pump beam from the defect as illustrated in Figure 3.

4. Summary

Single-beam PTM is demonstrated to be a sensitive and non-destructive evaluation tool for defect detection of optics for high power laser applications. Experimentally it is much simpler than the traditional two-beam PTMs, and more user-friendly. Because it is based on LMS it is also a dark-field technique for high-quality optical surfaces. Finally, under similar experimental condition single-beam PTM has a higher spatial resolution than the two-beam PTM based on optical diffraction and/or beam deflection effect.

The single-beam technique has been applied to both coated and bare substrates. By performing the scattering scan and the single-beam PTM map simultaneously the technique detects and differentiates between absorptive and non-absorptive defects. The phase signal of the single-beam PTM image reveals thermal inhomogeneities and/or the depth information of the absorbing defects.

While the preliminary studies performed in this work have shown the advantages of the single-beam technique, its applications to large-aperture optics and its sensitivity to sub-micron size defects are yet to be demonstrated. Furthermore, substantial modeling effort is needed to fully understand the single-beam PTM signal, particularly at high pump power. An inversion calculation should also be developed to allow identification of the detected defects.

5. Acknowledgments

This work is performed under the auspices of the U.S. Department of Energy by Lawrence Livermore National laboratory under contract No. W-7405-ENG-48. We thank Chrisopher Stolz, Robert Chow, and Diane Chinn for their support and fruitful discussions.

6. References

1. D. W. Camp, M. R. Kozlowski, L. M. Sheehan, M. Nichols, M. Dovik, R. Raether, I. Thomas, "Subsurface damage and polishing compound affact the 355-nm laser damage threshold of fused silica surfaces", in *Laser-induced damage in optical materials: 1997*, G. J. Exarhos, A. H. Guenther, M. R. Kozlowski, and M. J. Soileau, ed., Proc. SPIE **3244**, 356-364 (1998).
2. M. R. Kozlowski, J. Carr, I. Hutcheon, R. Torres, D. W. Camp, and Ming Yan, "Depth profiling of polishing-induced contamination on fused silica surfaces", in *Laser-induced damage in optical materials: 1997*, G. J. Exarhos, A. H. Guenther, M. R. Kozlowski, and M. J. Soileau, eds., Proc. SPIE **3244**, 365-369 (1998).
3. P. P. Hed, D. P. Edwards, and J. B. Davis, "Subsurface damage in optical materials: origion, measurement and removal", Appl. Opt. (1989).
4. M. D. Feit, J. Campbell, D. Faux, F. Y. Genin, M. R. Kozlowski, A. M. Robenchik, R. Riddle, A. Salleo, J. Yoshiyama, "Modeling of laser-induced surface cracks in silica at 355 nm", in *Laser-induced damage in optical materials: 1997*, G. J. Exarhos, A. H. Guenther, M. R. Kozlowski, and M. J. Soileau, eds., Proc. SPIE **3244**, 350-55 (1998).
5. R.J. Tench, R. Chow, M. R. Kozlowski, "Characterization of defect geometries in multilayer optical coatings", J. Vac. Sci. & Technol. A **12**, 2808-13, (1994).
6. S. Papernov, A.W. Schmid, J. Anzelotti, D. Smith, Z.R. Chrzan, "AFM-mapped, nanoscale, absorber-driven laser damage in UV high-reflector multilayers", in *Laser-induced damage in optical materials: 1995*, H. E. Bennett, A. H. Guenther, M. R. Kozlowski, B. E. Newnam, and M. J. Soileau, eds., Proc. SPIE **2714**, 384-94 (1996).
7. M. A. Paesler, P. J. Moyer, *Near-field optics* (John Wiley & Sons, Inc., New York, 1996).
8. M. Yan, S. Oberhelman, W. Siekhaus, Z. L. Wu, L. Sheehan, and M. Kozlowski, "Characterization of surface and subsurface defects in optical materials using near-filed evanescent wave", these proceedings.
9. P. A. Temple, "Total internal reflection microscopy: a surface inspection technique", Appl. Opt. **20**, 2656-64 (1981).

10. L. Sheehan, M. R. Kozlowski, D. Camp, "Application of total internal reflection microscopy for laser damage studies on fused silica", in *Laser-induced damage in optical materials: 1997*, G. J. Exarhos, A. H. Guenther, M. R. Kozlowski, and M. J. Soileau, eds., Proc. SPIE **3244**, 282-295 (1998).
11. M. A. Olmstead, N. M. Amer, S. Kohn, D. Fournier, and A. C. Boccara, "Photothermal displacement spectroscopy: an optical probe for solids and surcaes", Appl. Phys. A **32**, 141 (1983)
12. W. C. Mundy, R. S. Gughes, and C. K. Carlinia, "Photothermal defelcetion microscopy of thin film optical coatings", in *Laser-induced damage in optical materials: 1982*, H. E. Bennet, A. H. Guenther, D. Milam, and B. E. Newnam, eds., NBS SP **669**, 349-54 (1984).
13. Z. L. Wu, M. Thomsen, P. K. Kuo, C. Stolz, M. R. Kozlowski, "Photothermal characterization of optical thin film coatings", Opt. Eng. **36**, 251-262 (1997).
14. M. Commandre, P. Roche, "Characterization of optical coatings by photothermal deflection", Appl. Opt. **35**, 5021-34 (1996).
15. E. Welsch, D. Ristau, "Photothermal measurements on optical thin films", Appl. Opt. **34**, 7239-53 (1995).
16. J. Dijon, G. Ravel, and B. Andre, "Thermo-mechanical model of mirror laser damage at 1.06 μm", these proceedings.
17. Z. L. Wu, C. J. Stolz, J. M. Yoshiyama, and A. Salleo, "Characterization of fluence limiting defects in hafnia/silica multilayer coatings manufactured for the National Ignition Facility", paper presented at the 1998 Topical Meetings of Optical Society on Optical Interference Coating, June 7-12, 1998, Tucson, Arizona.
18. Z. L. Wu, M. D. Feit, Mark R. Kozlowski, A. M. Rubenchik, and L. Sheehan, "Laser modulated scattering as a nondestructive evaluation tool for optical surfaces and thin film coatings", these proceedings.
19. The estimation of the dimension was made using the theory described in reference 11.
20. A. M. Rubenchik, private communications.
21. Craig F. Bohren and Donald R. Huffman, *Absorption and scattering of light by small particle* (John Wiley & Sons, New York, 1983).
22. When the thermal diffusion length is much larger than the thickness of the thin film coating, the coating sample is generally considered thermally thin and the amplitude of the photothermal signal is primarily determined by the absorption of the coating and the thermal properties of the substrate.